Representation of the stratosphere in ECMWF operations and ERA-40

Adrian Simmons

European Centre for Medium-Range Weather Forecasts

1. Introduction

The model and data assimilation system used at ECMWF for operational analysis and prediction since 1999, and for the ERA-40 reanalysis for the period 1957-2002, has a comprehensive representation of the stratosphere. It includes ozone as a prognostic variable in addition to the primary dynamical variables and specific humidity. The operational data assimilation uses radiosonde wind and temperature data in the middle and lower stratosphere, and AMSU-A microwave satellite sounding radiances that span the whole stratosphere. ERA-40 also utilized SSU, MSU and HIRS data (available since late 1978) and VTPR data (from 1973 to 1978).

In this presentation several aspects of the representation of the stratosphere by either the operational ECMWF forecasting system or the ERA-40 system are discussed. Some of the examples presented indicate significant progress and high current levels of skill, whereas others highlight some remaining substantial problems. Aspects of the numerical formulation of the ECMWF model are discussed further in Untch's presentation to this workshop. Morcrette discusses radiative aspects. The assimilation of radiance data is discussed in the presentation by McNally, and the ozone data assimilation is described by Dethof.

2. Configurations of the ECMWF forecasting system

Figs. 1 to 3 illustrate how the vertical resolution has evolved over the years since 1983, with the top level moving from 25hPa to 10hPa in 1986, and then to 0.1hPa in 1999 for data assimilation and deterministic forecasting. The number of levels above 100hPa has correspondingly increased from 2 to 25. Level spacing around the tropopause has been reduced from about 50hPa to 20-30hPa. Over the same period the model's horizontal grid-length has been reduced by a much larger factor, from about 200km to about 40km. Figs. 2 and 3 also provide the dates of the key analysis changes from OI to 3D-Var and then to 4D-Var, and basic information on the configurations of the forecasting system used for ECMWF's two reanalyses, ERA-15 (from 1979-1994, using 31-level vertical resolution) and ERA-40 (from 1957 to 2002, using 60-level vertical resolution).

3. Time series of forecast verification statistics

Time series of forecast verification statistics are presented in Figs. 4 to 6. Fig. 4 shows substantial reductions over the years in the error of operational 50hPa wind forecasts over the northern hemisphere, marking in particular the reductions in error (measured by verification against analyses) associated with the increases in stratospheric resolution made in 1986 and 1999, and with the introduction of 3D-Var in 1996. The flat reference curve provided by the one-day forecasts from ERA-40 indicates that these operational forecast improvements have come almost entirely from changes made to the forecasting system rather than from changes in the observing system. Fig. 5 repeats the time series from Fig. 4 and adds the corresponding plots for winds in the southern hemisphere and temperatures in both hemispheres. All plots show stable ERA-40 performance and a reduction over time in operational errors. Temperature scores show a much less marked impact of 3D-Var than is seen for wind scores.

4. Analysis increments

Fig. 6 shows that verification against radiosondes does not exhibit the sharp reduction in forecast error following the introduction of 3D-Var that is suggested by the verification against analyses. The explanation is that the apparent reduction in wind-forecast error as measured by verification against analyses is in fact not due to a significant reduction in forecast error but rather to a change in the verifying analyses. The 3D-Var analysis draws much less closely to radiosonde wind data than the OI analysis (as discussed by Andersson *et al.*, 1998, *Quart. J. Roy. Meteor. Soc.,* 124, 1831-1860). This is reflected in much smaller analysis increments for wind in ERA-40 (which used 3D-Var) than ERA-15 (which used OI). This can be seen in Fig. 7, which also shows that temperature increments from the two reanalyses are similar in magnitude. Another consequence is smoother, more coherent derived potential-vorticity fields. Fig. 8 is an example for the 850K surface showing the southern polar vortex and bands of material stripped from it. Small-scale structure is evident within the core of the vortex; this is generated by the flow changes produced by the assimilating model's parametrization of gravity-wave drag.

5. The southern hemisphere sudden warming in September 2002

The case shown in Fig. 8 depicts the polar vortex a few days before it split in late September 2002 in a way never-before observed. Illustrations of the event in terms of 850K potential vorticity and specific humidity, and 10hPa height, are shown in Figs. 9 and 10, for analyses and five-day forecasts. Further indications of the accuracy of analyses and forecasts for the period leading up to the event are given in Figs. 11 to 13. For discussion of these and additional results, see Simmons *et al.* (2003, *ERA-40 Project Report No. 5*).

6. Temperature trends and low-frequency variability in ERA-40

Fig. 14 shows how the ERA-40 reanalysis reproduces the trend of lower stratospheric cooling that has been identified in observational studies of the radiosonde and MSU data record. ERA-40 captures the warm periods following the volcanic eruptions of Agung in 1963, El Chichon in 1982 and Pinatubo in 1991, improving considerably with regard to ERA-15 for the latter. The warm period in 1975/76 is, however, spurious. It arises from a problem in bias correction of the VTPR data from the NOAA-3 satellite. ERA-40 results prior to 1979 must more generally be viewed with caution. No bias correction was applied to radiosonde data for this period, which is likely to have introduced a warm bias in the analyses. Conversely, the reanalyses are too cold in winter and spring over Antarctica in the early years when there were insufficient data to correct a pronounced model bias.

Temperatures near the tropical tropopause also show sensitivity to assimilation method and radiance bias correction. The time series at 100hPa shown in the upper panel of Fig. 15 compare ERA-40 with ERA-15 and recent operational results. Agreement is close from 1989 to 1997. From 1979 to 1988 the ERA-40 analyses are generally colder than their ERA-15 counterparts and for the most part colder than in earlier and later periods of ERA-40. The reason for this behaviour remains to be determined, but radiance bias correction appears to be a factor. The ERA-40 analyses do not show the colder temperatures seen in ECMWF operations from 1998 onwards, which follow the operational introduction of the 4D-Var analysis and a major parametrization revision. It is the ERA-40 analyses that fit radiosonde data better in this period, as can be seen in the bottom left panel. The bottom right panel shows that it is not only the ECMWF operational system that is prone to shifts in analysed temperatures near the tropical tropopause.

An example of ERA-40 and ERA-15 fits to (uncorrected) 00UTC and 12UTC radiosonde data from a tropical station (Pago Pago International Airport) is presented in Fig.16 for the period from 1979 onwards. At 12UTC, ERA-40 fits the sonde data well from 1987 onwards, but tends to be colder than the sonde data

before then during the austral winter. Sonde temperatures at 00UTC are warmer than ERA-40 before 1996, but are warmer also than the 12UTC sonde temperatures. The likely explanation for this is that the sonde data before 1996 have a warm bias at 00UTC (close to local noon) that is corrected when they are used in ERA-40. ERA-15 tends to be too warm at 12UTC and follows the 00UTC data more closely, suggesting that the sonde bias correction was less effective in the earlier reanalysis. Such ERA-40 fits will in due course be diagnosed for all assimilated data; for the time being the example in Fig. 16 suggests that with regard to the 100hPa temperature time series shown in Fig. 15, the truth may lie somewhere between the ERA-15 and ERA-40 curves for the period from 1979 to 1989.

Fig. 17 shows time series of monthly- and global-mean temperatures at 1hPa and 3hPa. At 3hPa, results are very sensitive to the assimilation of radiance data from the high-sounding channels of the VTPR (1973-78), SSU (1979 onwards) and AMSU-A (1998 onwards) instruments, and in particular to the bias corrections that are applied to these data. The bias corrections applied from 1973 to early 1981 ensured that the analysis matched the mean temperature produced by the assimilating model in the pre-satellite period, apart from the clear problem stemming from erroneous bias-correction of VTPR data from NOAA-3 in 1975 and 1976, which is much more pronounced at 3hPa (and at 1hPa) than at the 70hPa level illustrated earlier. ERA-40 production in fact began with the period from 1989 onwards, and bias corrections were chosen initially to ensure continuity with current ECMWF operations. The bias corrections applied from early 1981 onwards were chosen to match the corrections that had been applied from 1989 onwards. The variations between 1981 and 1989 reflect further difficulties arising from failures of particular SSU channels and the general difficulty of ensuring consistent bias correction. A study of stratospheric climatologies (Randel, W., M.-L. Chanin and C. Michaut (Eds.),2002, *SPARC intercomparison of middle atmosphere climatologies.* WCRP – 116, WMO/TD – No. 1142, Sparc Report No. 3) indicates that the ERA-40 analyses have a cold bias of a few degrees in the upper stratosphere from 1989 to 1998, and by implication the analyses prior to early 1981 exhibit a warm bias due to a systematic error of the background forecast model.

The 3hPa level illustrated in Fig. 17 is particularly sensitive to bias-correction difficulties. The 3D-Var analysis scheme used for ERA-40 is prone to fit the measured radiances (which are sensitive to distributions of temperature over relatively deep stratospheric layers) by introducing oscillatory temperature structures (peaking close to 3hPa) with vertical scales finer than those to which the measured radiances are most sensitive. The problem (which is discussed further in McNally's presentation) is most marked in polar regions, particularly the Antarctic, and particularly later in the period when both SSU and AMSU-A data are assimilated. It is illustrated in Fig.18, which presents a meridional cross-section of the zonal-mean temperature difference between the analyses for January 1989 and January 1981. The major SSU bias-correction change was made shortly after January 1981.

There is a further noteworthy difference between January 1981 and January 1989. SSU data from two satellites were available for January 1981, whereas data from only one satellite were available for the later month. Assimilation of upper stratospheric temperature information from a single sun-synchronous satellite by the six-hourly 3D-Var system used for ERA-40 was especially problematic, as it was difficult to distinguish a background error in the semi-diurnal tide from an overall bias in the background forecast. Fig. 19 illustrates how the analysis increments in 3hPa temperature for January 1989 have a substantial semi-diurnal signal, with large cooling increments (along the satellite tracks) that not only compensate for the warm model bias but also compensate for the warming introduced six hours earlier by the analysis system (via its structure functions). The corresponding increments for January 1981 shown in Fig. 20 are much smaller and less structured. As noted above, the different bias correction applied to the SSU data for this month results in little or no overall correction of the warm model bias.

7. Humidity and ozone in ERA-40

Use of the three-dimensional velocity fields from ERA-40 to drive long-term chemical transport models has been found to produce an "age of air" in the stratosphere that is much too young (van Velthoven, personal communication), indicating that the Brewer-Dobson circulation in the ERA-40 data assimilation is considerably too strong. One consequence of this that can be seen directly is a too rapid "tape-recorder" effect in the tropical stratospheric humidity fields (Oikonomou, personal communication). No change to the stratospheric humidity is made by the ERA-40 analysis other than removal of any supersaturation, so the distribution of stratospheric humidity in ERA-40 is determined primarily in the sequence of six-hour background forecasts, by tropospheric exchange, by the upper-level moistening due to parametrized methane oxidation and by advection. Fig. 21 presents a pressure/time cross-section of the monthly- and zonal-mean specific humidity analysis at the equator. Relatively dry air introduced at the tropical tropopause in boreal winter, and relatively moist air introduced in boreal summer, spread upwards to reach above 10hPa in well under a year. Simulations with the ECMWF model, either as reported earlier by Simmons *et al.* (1999, *Quart. J. Roy. Meteor. Soc.*, **125**, 353-386) or run using a version more similar to that used for ERA-40, tend to produce too rapid an upward transfer in the tropics, but transfer is faster still in the ERA-40 data assimilation. It thus appears that the assimilation of observations disrupts the model's balance in such a way as to increase an already too-strong upward transport.

Considerable interannual variability can be seen in Fig.21. From the above discussion, some of this variability may well be related to changes in the availability or bias-correction of stratospheric observations, but there is also variability in the input at the tropical tropopause, particularly in the degree of summertime moistening. The slow timescale of changes in tropical stratospheric humidity (albeit faster in the analyses than in reality) is reflected in Fig. 21 in clear discontinuities in the time series in the middle stratosphere, associated with the fact that ERA-40 was run as a number of separate production streams, rather than as a single stream from 1957 to 2002.

A brief discussion of the comparison of ERA-40 analyses with a climatology from UARS data, with remarks in particular on the parametrization of methane oxidation, is given by Simmons (2002, contribution to *ERA Project Report No. 3*).

Ozone data assimilation is discussed elsewhere in these proceedings, but it is appropriate to include one figure here. Fig. 22 compares monthly-mean total column ozone from ERA-40 with corresponding monthly means of (non-assimilated) ground-based measurements from two sites, Barrow and Bismarck, located respectively at polar and middle northern latitudes. Ozone retrievals from TOMS and SBUV satellite measurements were assimilated in ERA-40 from 1979-1988 and from 1991 to 2002, and for these years the ERA-40 analyses match well the independent ground-based measurements, capturing interannual variability but with a small general underestimation of summertime minima. In addition, the observations from Bismark in the 1960s are reproduced well by ERA-40, even though no ozone data was assimilated for this period, and values for Barrow for the same period are consistent with the values measured in the 1980s. Conversely, there is a clear overestimation of wintertime values in the period from 1973 to 1978 and in 1989/90 when either VTPR or TOVS radiance data were assimilated to adjust stratospheric temperatures but no ozone data was assimilated. Wintertime ERA-40 values are relatively high also in the pre-satellite years of 1969, 1970 and 1971, although the same is true, but to a lesser extent, for the observations from Bismarck for 1969 and 1970. The indication from these results is that wintertime ozone transport is too strong in ERA-40, especially when radiance data influence the stratospheric analysis, but that its effect is compensated (at least as regards the total column value) when the TOMS and SBUV retrievals are assimilated.

8. Quasi biennial oscillation in ERA-40

As illustrated by Untch (2002, contribution to *ERA Project Report No. 3*) and in the SPARC intercomparison of climatologies referenced earlier, the quasi-biennial oscillation (QBO) of zonal wind in the tropical stratosphere is handled well in ERA-40. The SPARC comparison also shows that there is reasonable agreement between the semi-annual oscillation (SAO) at 1hPa in the ERA-40 analyses for 1989-1995 and the SAO as depicted by a limited climatology of rocketsonde data.

The upper panel of Fig. 23 shows that ERA-40 draws closely to the 30hPa radiosonde data from Canton Island. The period chosen is from 1958 to 1963, which means that the earliest of these observations were the same ones that led Reed and Ebdon to make the first identifications of the QBO more than 40 years ago. ERA-40 not only reproduces the value at the station itself, but also produces similar winds in the zonal mean. This is not the case in the example shown in the lower panel, for Gan from 1973 to 1975. Here the analysis draws to the quite marked short-period fluctuations in the data at the location of the station itself, but these fluctuations are not represented in the zonal mean. It is noteworthy that the fluctuations disappear almost completely and station values are reproduced in the zonal-mean analysis only during the period of the GATE experiment in 1974, when a special effort was made to collect comprehensive good quality radiosonde data throughout the equatorial zone for study of the tropical stratosphere.

Results at the higher levels of 10hPa and 5hPa are presented for Singapore in Fig.24, for the period 1989 to 1993. 10hPa was the top level of the ERA-15 reanalysis, and the local and zonal-mean ERA-40 analyses can be seen to fit the observations at this level very much better than the zonal mean ERA-15 analyses did. Both QBO and SAO signals are seen in the 5hPa time series, and ERA-40 again reproduces the observed variations well, although at this level there is a larger difference between the analysis at the station location and the zonal mean.

9. Concluding remarks

The representation of the stratosphere in the ECMWF forecasting system has been refined significantly over the years, particularly by the major increase in resolution introduced in 1999. This has been reflected both in substantially improved operational stratospheric forecasts and in improved reanalyses of observations of low-frequency variations in tropical stratospheric winds and lower-stratospheric temperature. A recent highlight was the highly accurate operational prediction of the splitting of the southern hemisphere winter vortex that occurred in September 2002, an event not previously observed in this hemisphere.

Several substantial deficiencies in performance have nevertheless been presented here. They arise predominantly from biases, both in the model (where they may stem from difficulties in the treatment of radiation, gravity-wave drag and upper boundary conditions) and in the satellite-radiance and radiosonde-temperature data that are assimilated using the model. Several apparent consequences of the systematic mismatch between model and observations in data assimilation cycles have been illustrated: oscillatory temperature increments that spread below the main region of model bias in the upper stratosphere (especially in polar regions), difficulties in handling tides, and circulation adjustments that increase constituent transport rates. Problems have been particularly pronounced for ERA-40, partly because the 3D-Var assimilation system it used is more prone to them than the operational 4D-Var system, and partly because of the inhomogeneity of the stratospheric observing system over the period of the reanalysis.

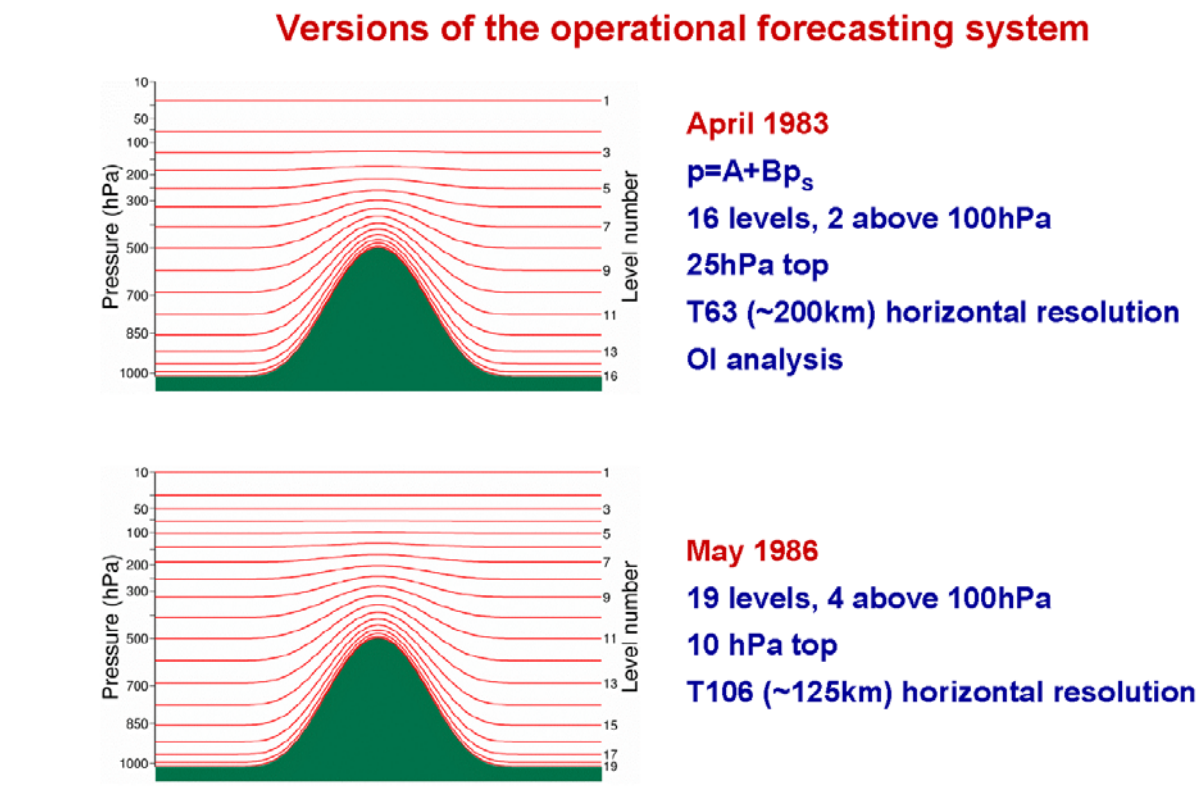

Figure 1: Aspects of the configurations of the ECMWF forecasting system introduced in April 1983 and May 1986.

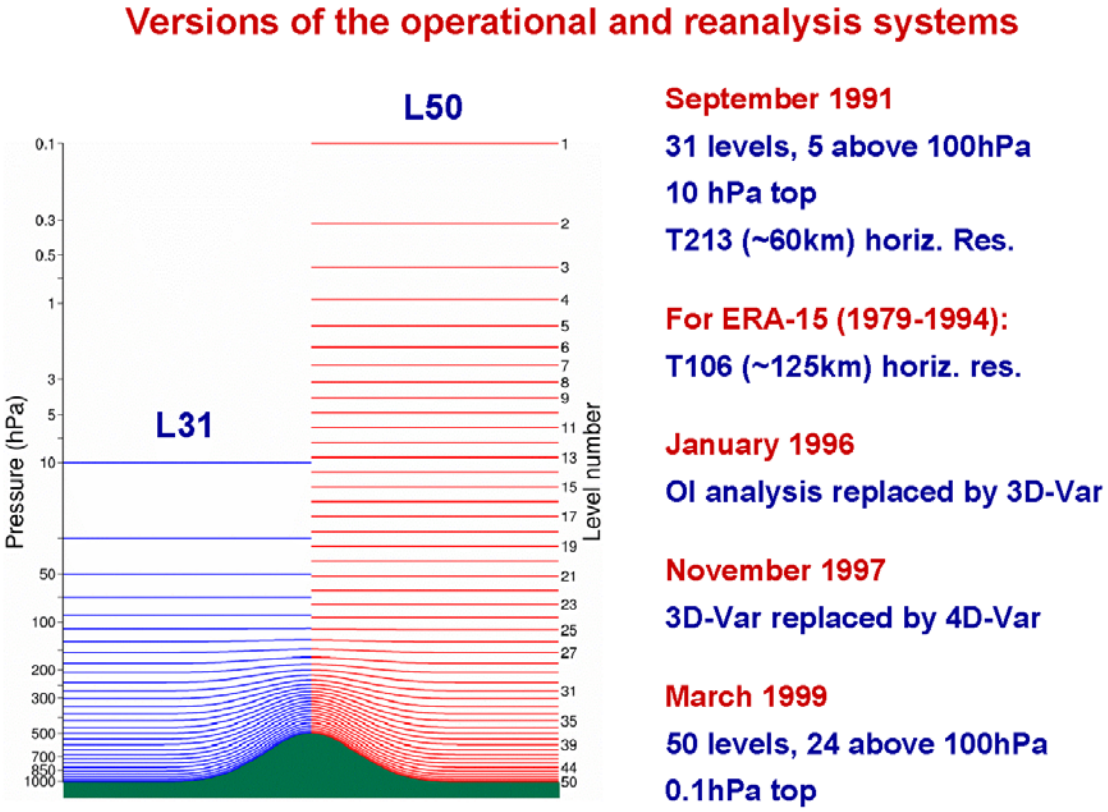

Figure 2: Aspects of the configurations of the ECMWF forecasting system introduced from September 1991 to March 1999.

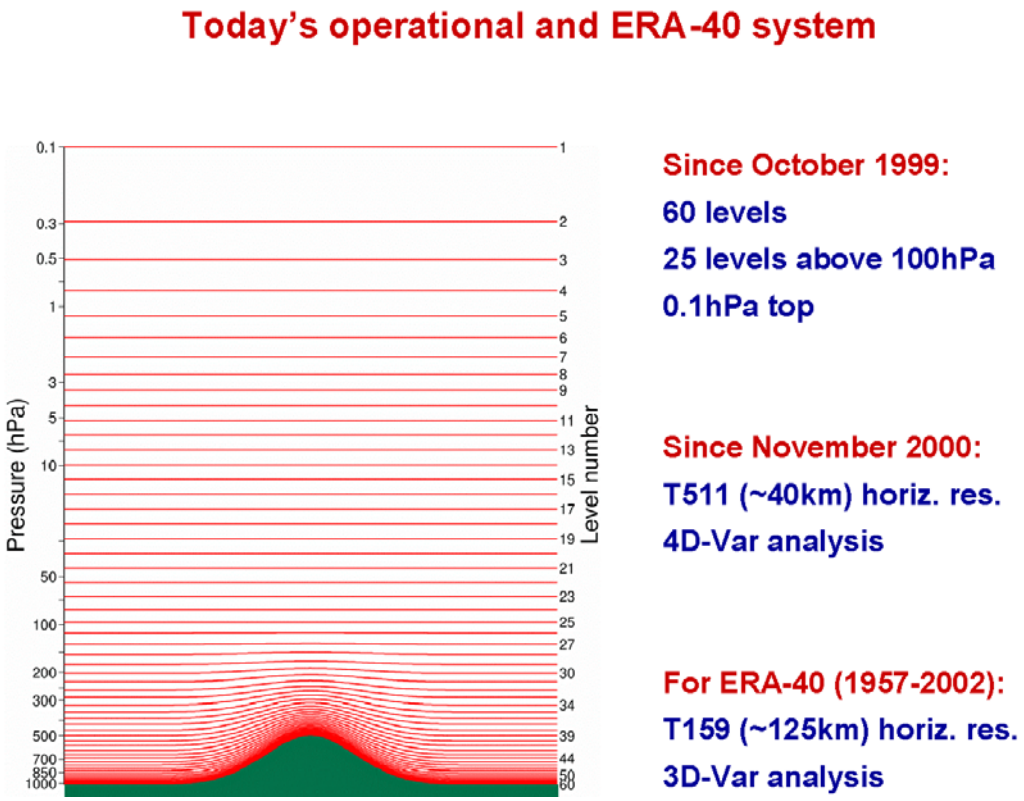

Figure 3: Aspects of the current operational and ERA-40 configurations of the ECMWF forecasting system.

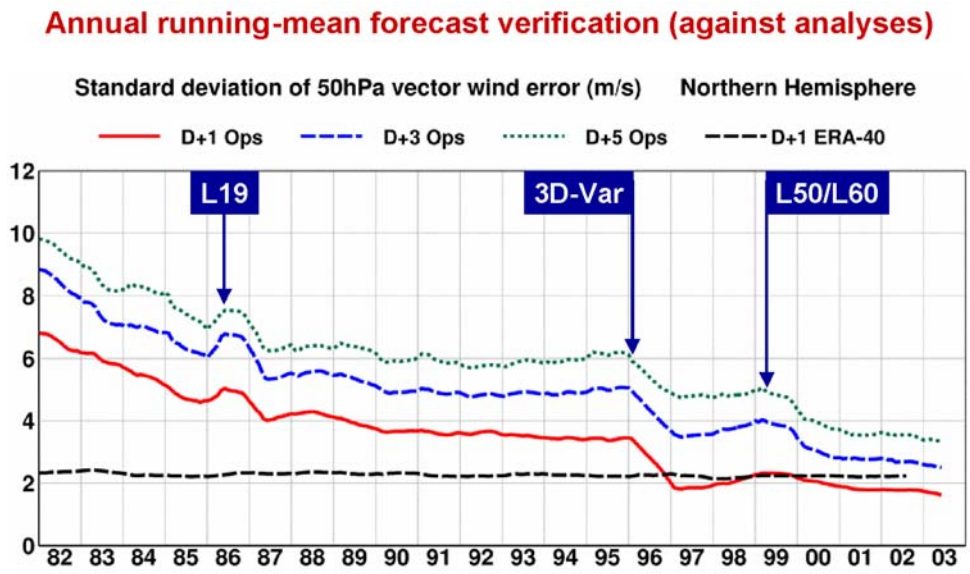

Figure 4: Time series of annual running mean standard deviations of operational one-, three- and five-day extratropical northern hemisphere forecasts of 50hPa vector wind carried out from 1 January 1981 to 31 May 2003. The time series for one-day ERA-40 forecasts from 1 January 1981 to 31 August 2002 is also shown. Forecasts are verified against corresponding analyses. Values plotted for a particular month are averages over that month and the 11 preceding months, so that the effect of a forecasting-system change introduced in that month is seen from then onwards.

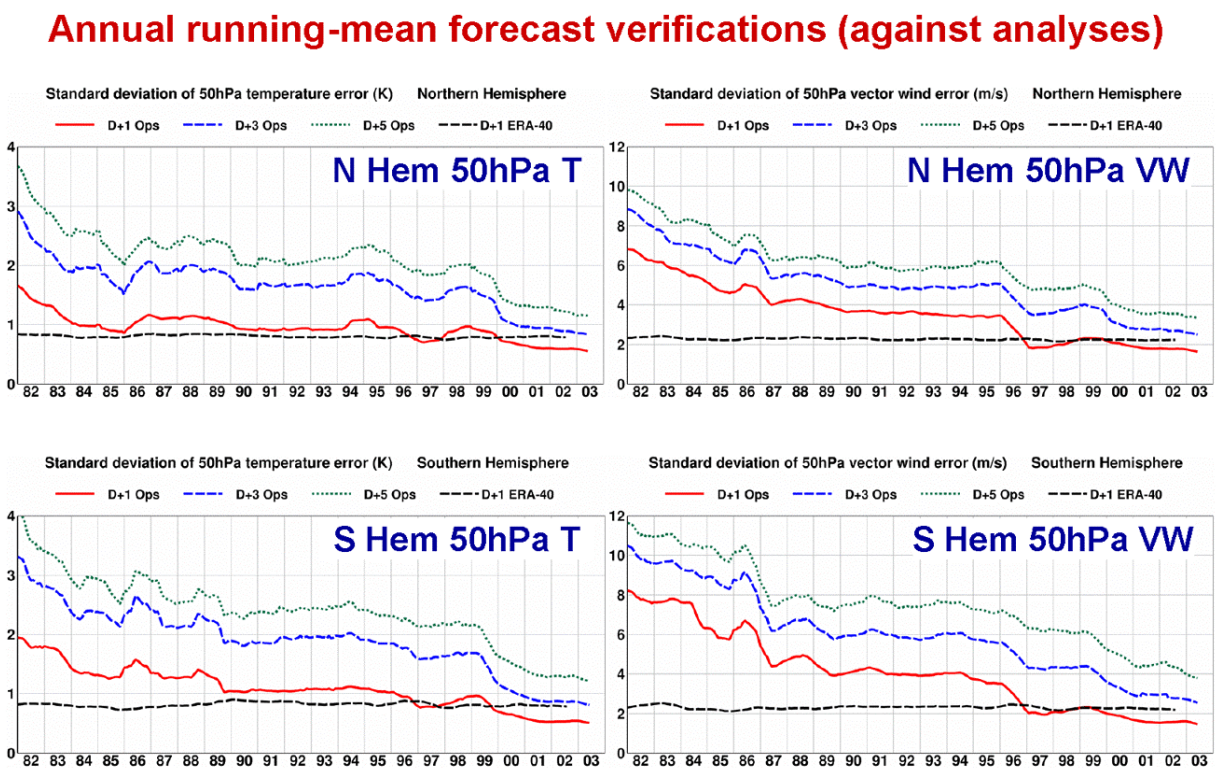

Figure 5: As Fig. 4, but showing standard deviations of 50hPa temperature and vector-wind forecasts for the extratropical northern and southern hemispheres.

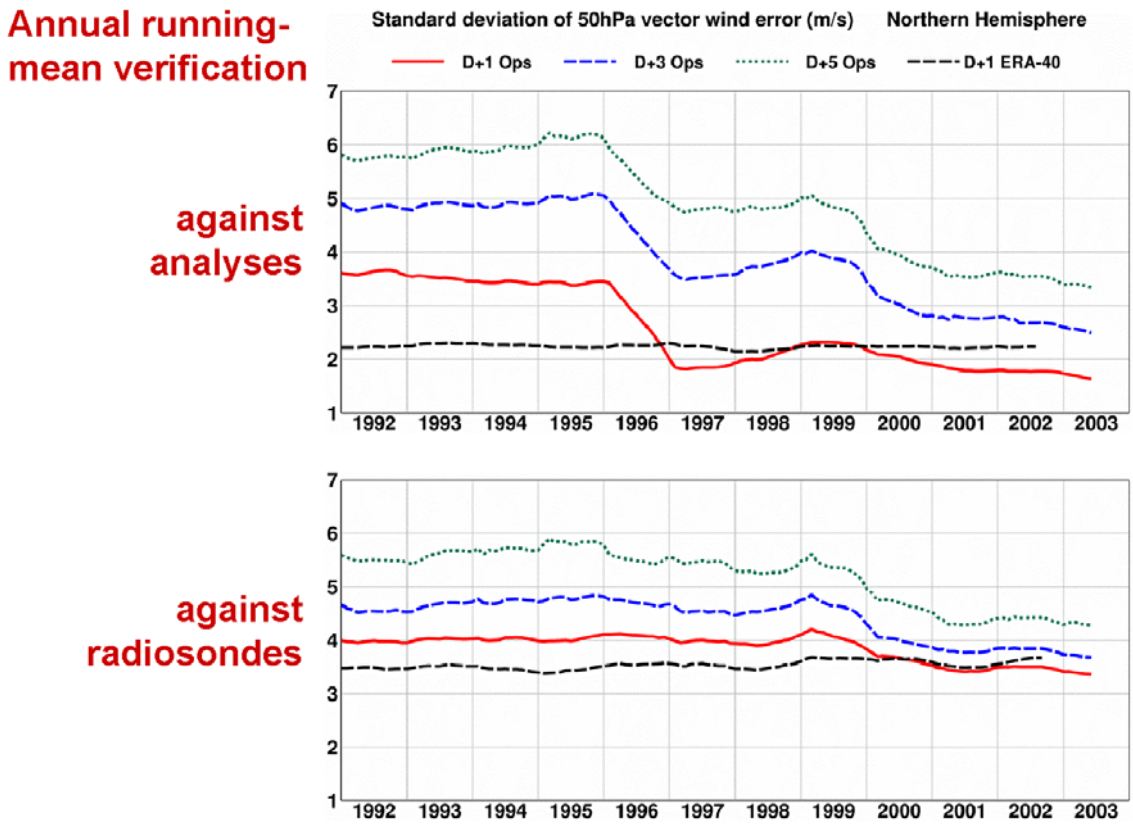

Figure 6: As Fig. 4, but comparing verifications against analyses and radiosonde data, for forecasts from 1 January 1991 onwards.

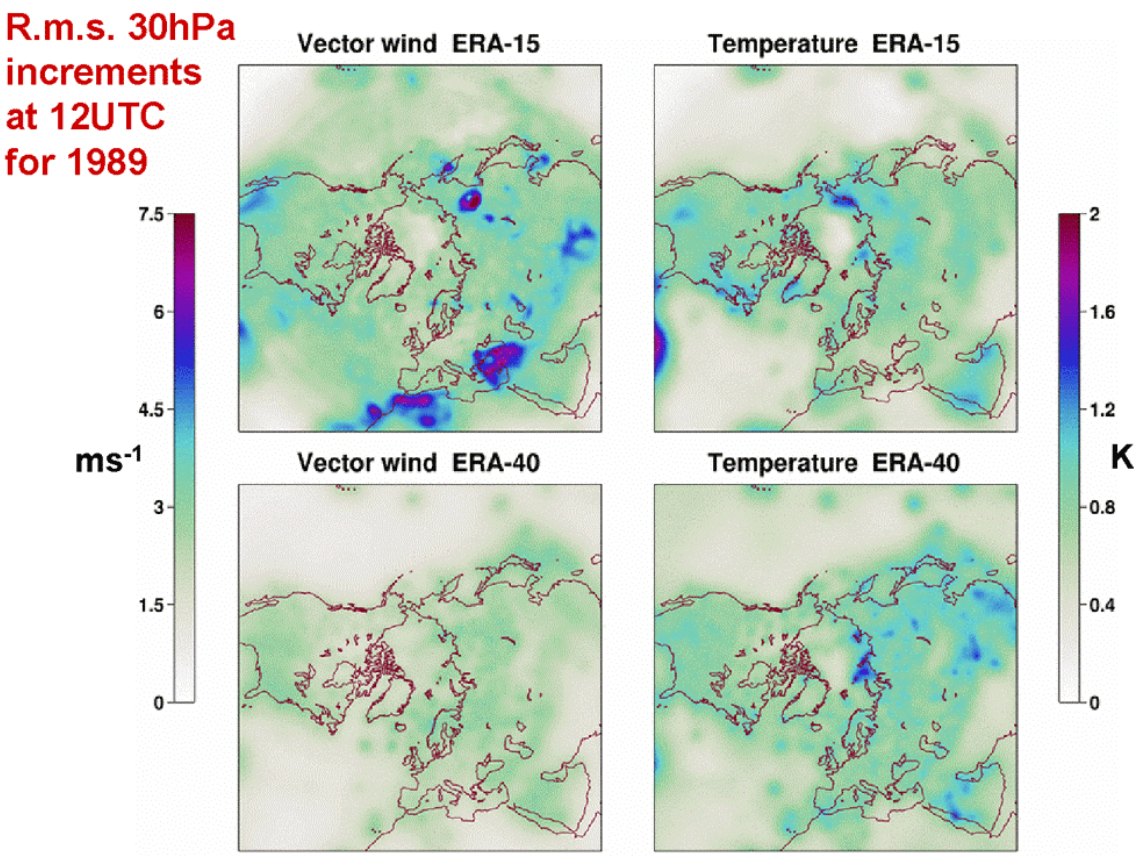

Figure 7: Root-mean-square northern hemisphere analysis increments in 30hPa vector wind and temperature for ERA-15 and ERA-40, computed for the year 1989.

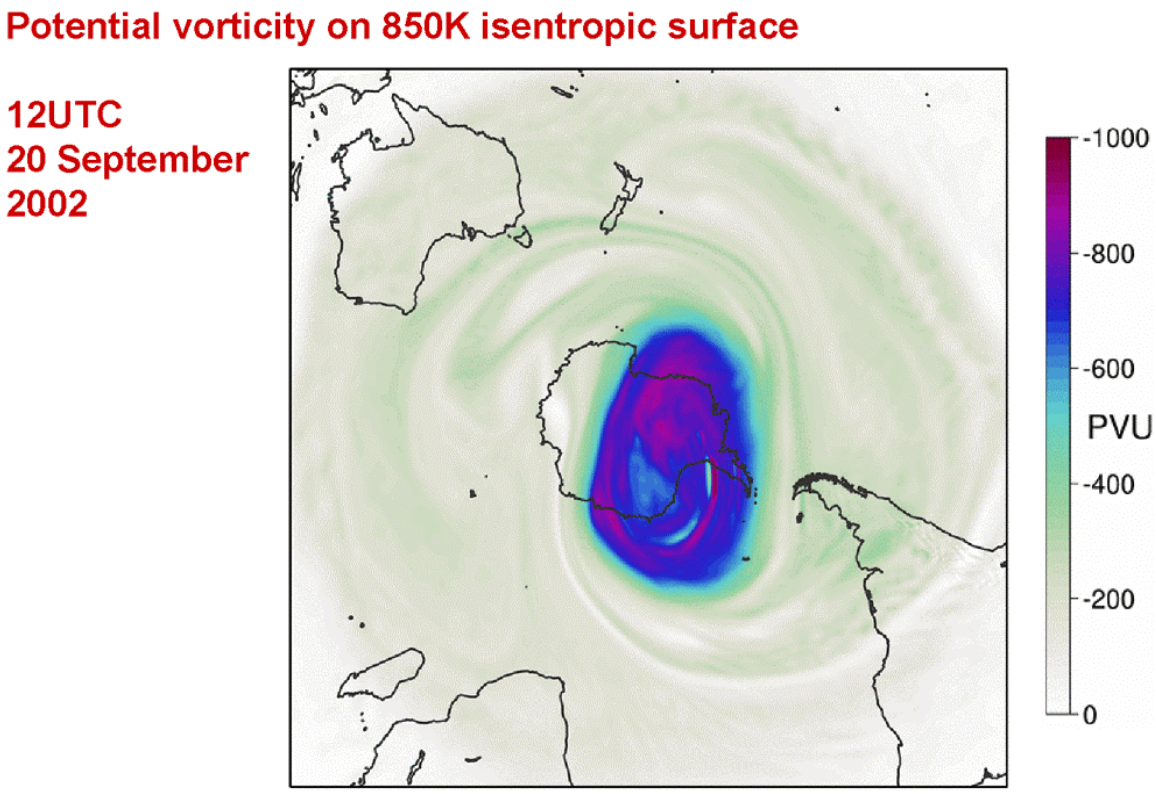

Figure 8: Potential vorticity on the 850K isentropic surface for the southern hemisphere derived from an analysis for 12UTC 20 September 2002 produced using the version of the ECMWF forecasting system introduced into operations on 14 January 2003.

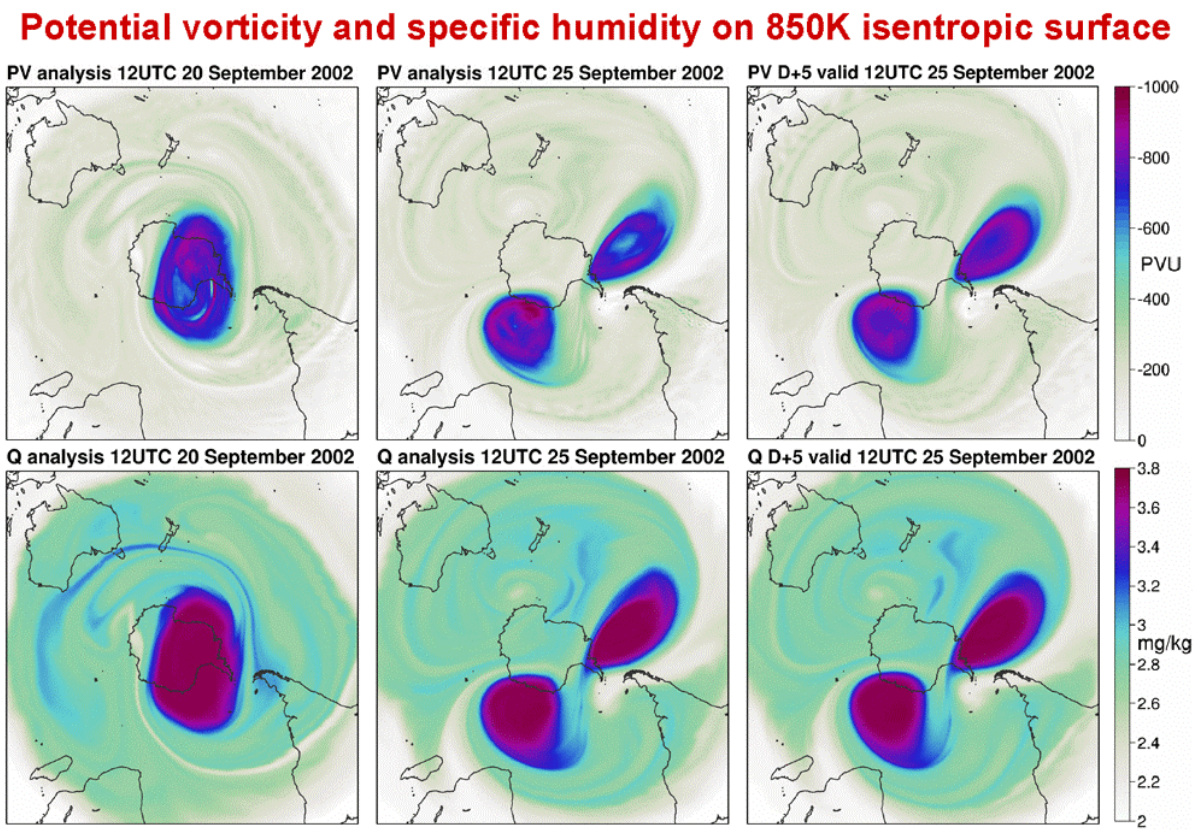

Figure 9: As Fig 8, but showing also the analysis and five-day forecast fields of 850K potential vorticity valid 12UTC 25 September 2002. Corresponding 850K specific humidity fields are also shown.

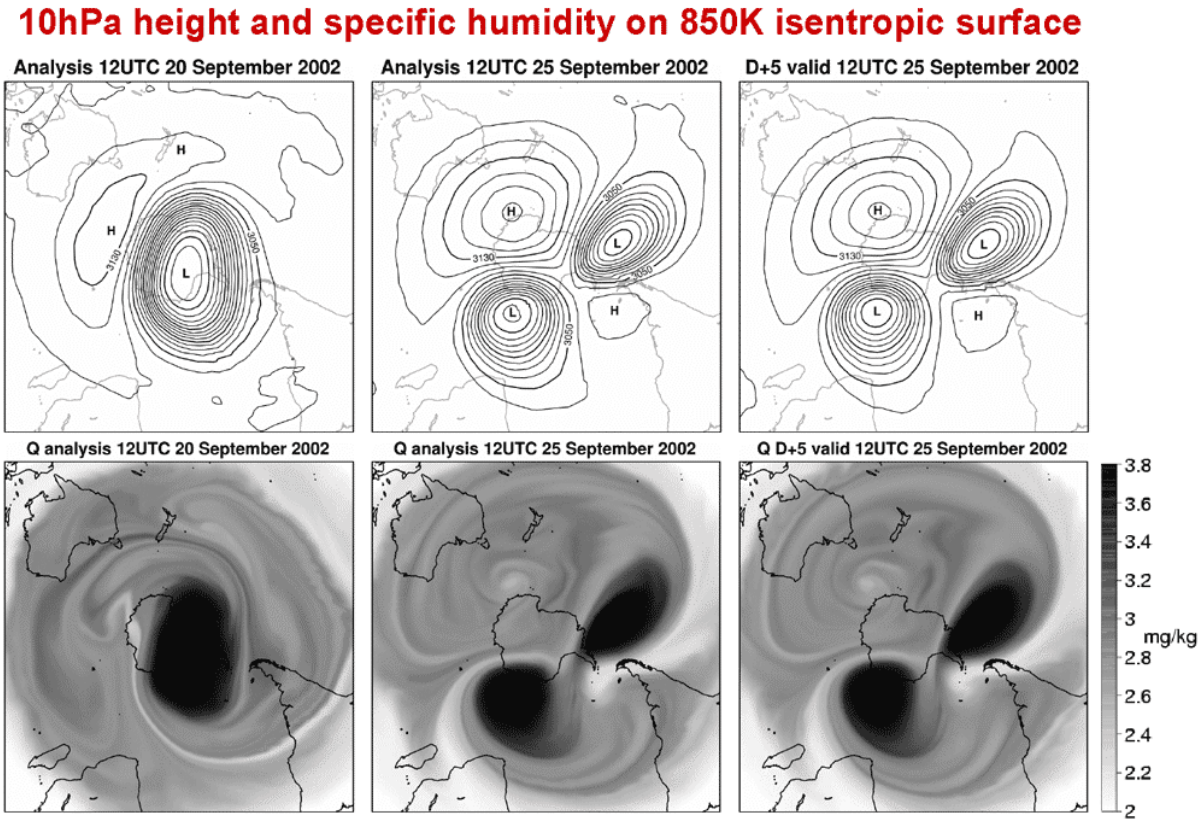

Figure 10: As Fig. 9, but showing 10hPa height (contour interval 20dam) and 850K specific humidity.

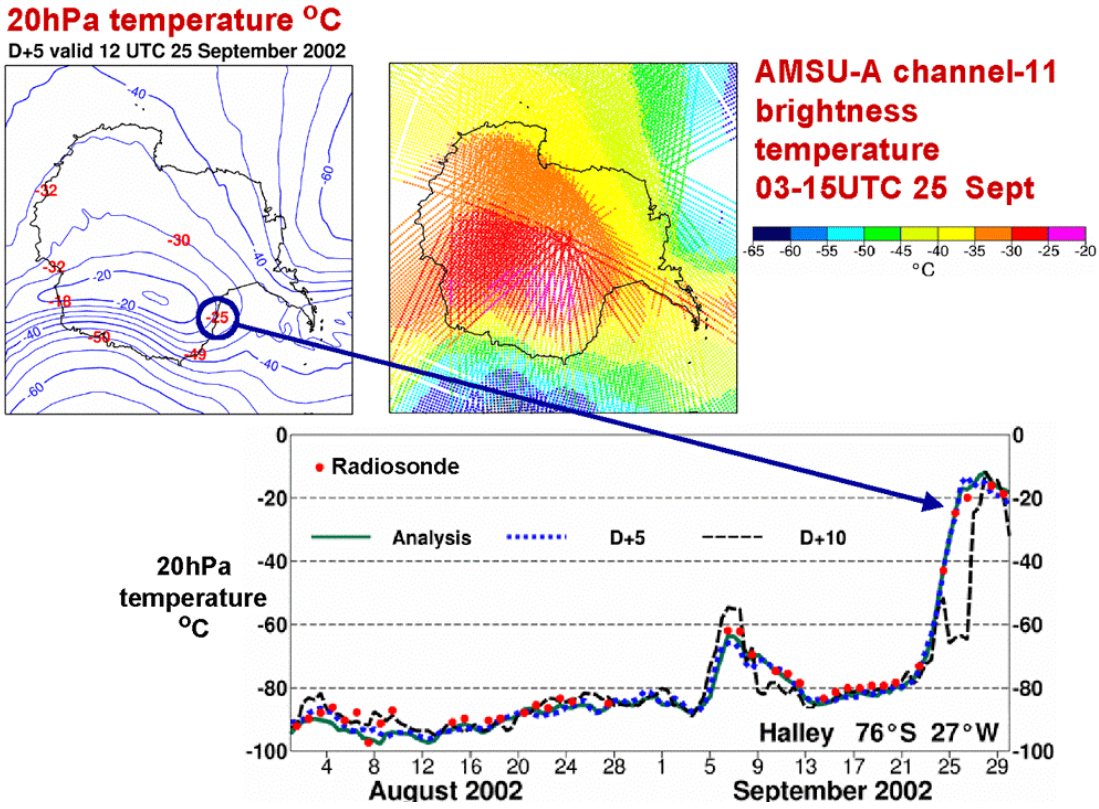

Figure 11: Aspects of the comparison of 20hPa temperature analyses and forecasts with observations. Maps show the five-day forecast valid 12UTC 25 September 2002 with superimposed verifying radiosonde observations, and the channel-11 AMSU-A brightness temperatures for the corresponding 12-hour assimilation window. A time series of radiosonde, analysis and forecast values is shown for the Halley radiosonde station.

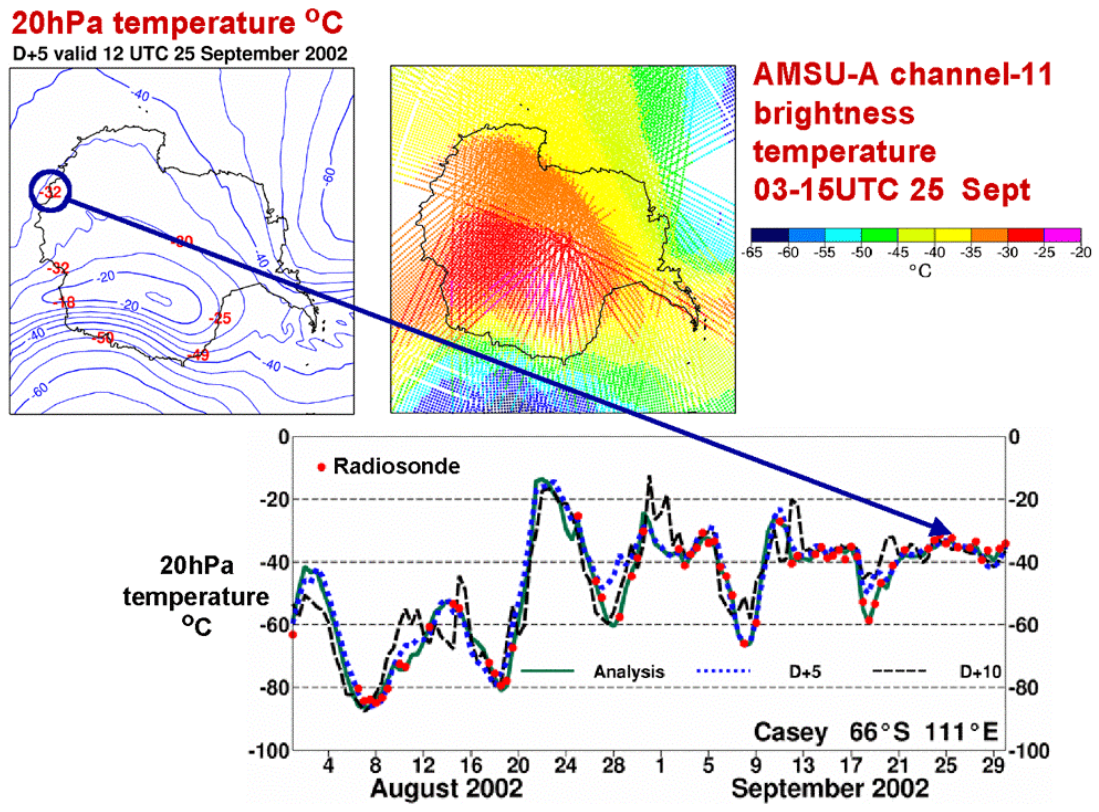

Figure 12: As Fig. 11, but showing time series for radiosonde station Casey.

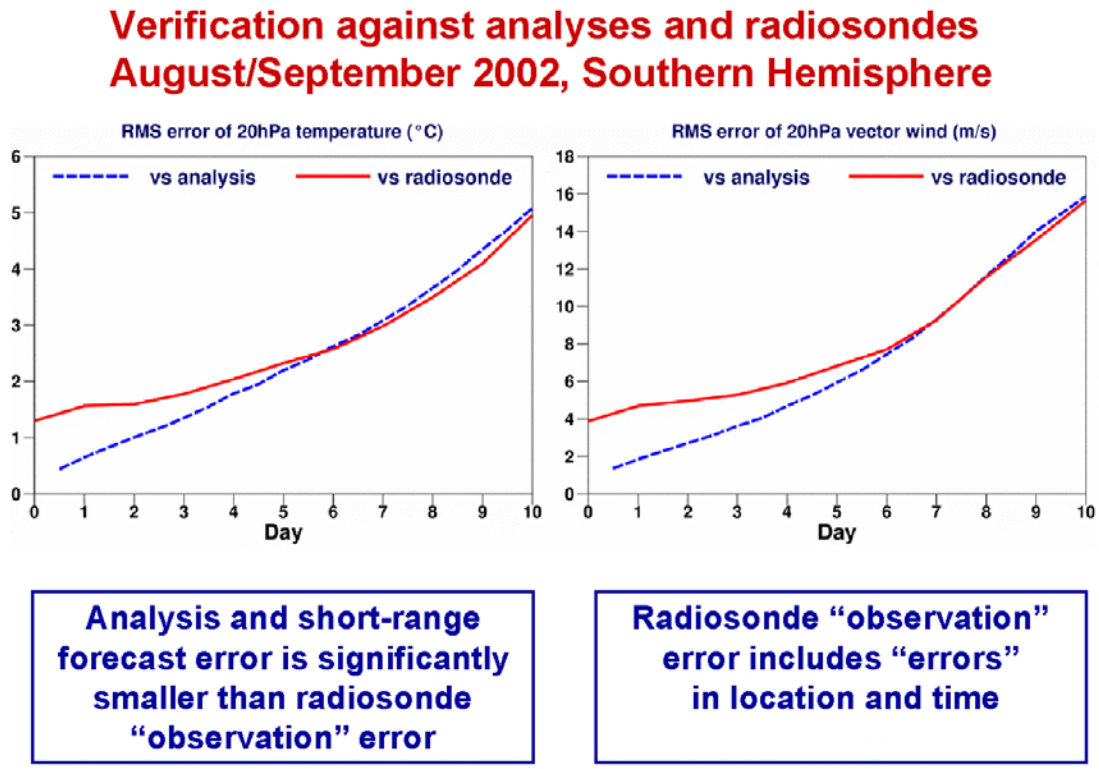

Figure 13: Root-mean-square errors of 20hPa temperature and vector-wind forecasts for the extratropical southern hemisphere, averaged for start-dates from 1 August to 30 September 2002, with verification against analyses and 12UTC radisondes.

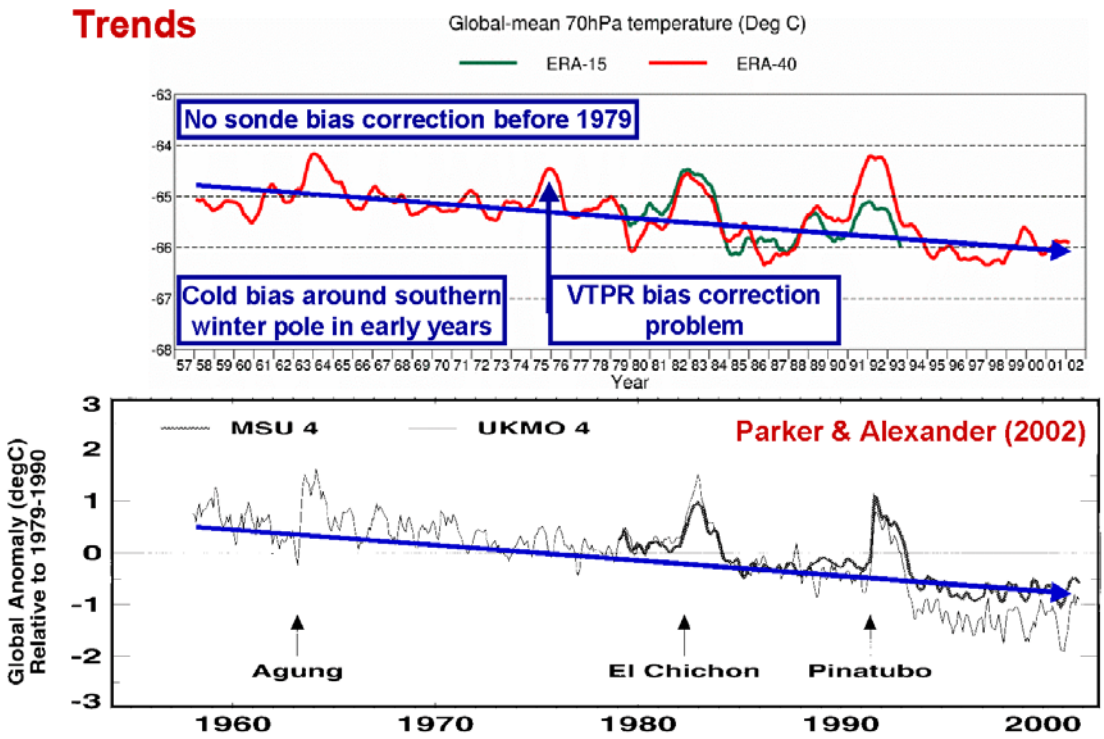

Figure 14: Time series of annual running means of globally averaged 70hPa temperatures from ERA-40 and ERA-15, compared with time series of anomalies in MSU-4 retrievals and equivalent radiosonde temperatures, from Parker and Alexander (2002, Weather, 57, 328-340).

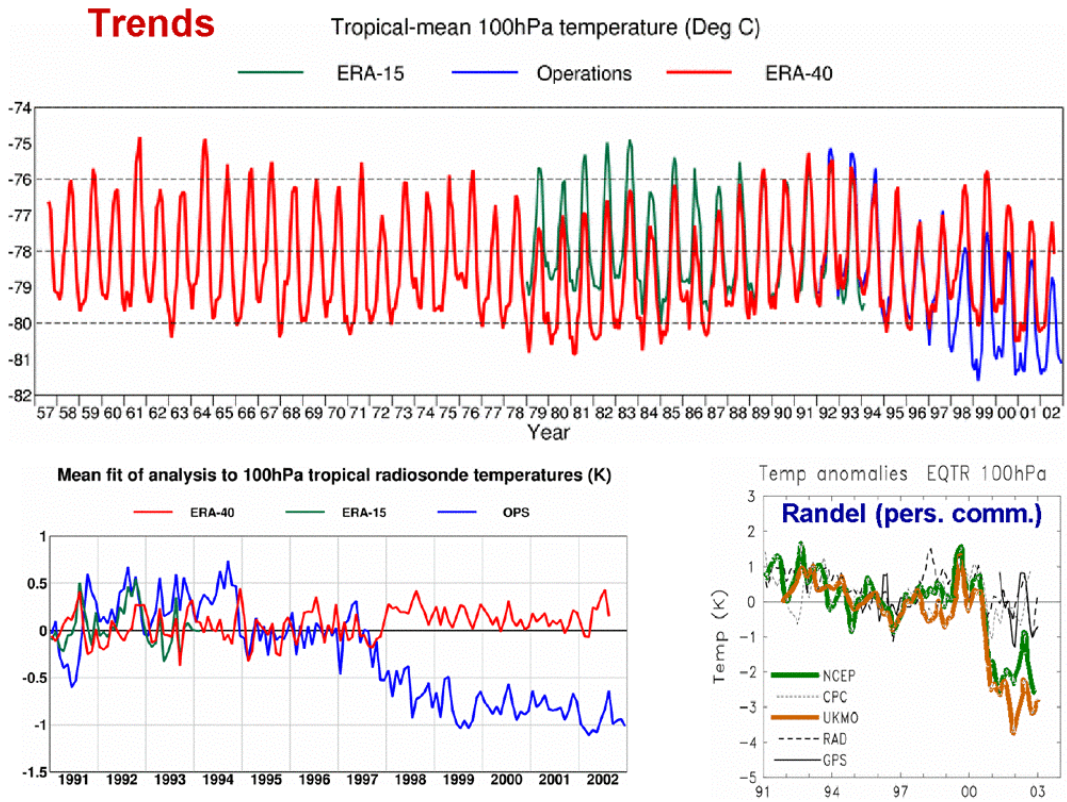

Figure 15: Time series of monthly- and tropical-mean 100hPa temperatures from ERA-40, ERA-15 and recent ECMWF operations, monthly-mean fits of ERA-40 and operations to tropical radiosondes, and equatorial temperature anomalies from NCEP and Met Office analyses (from W. Randel, personal communication).

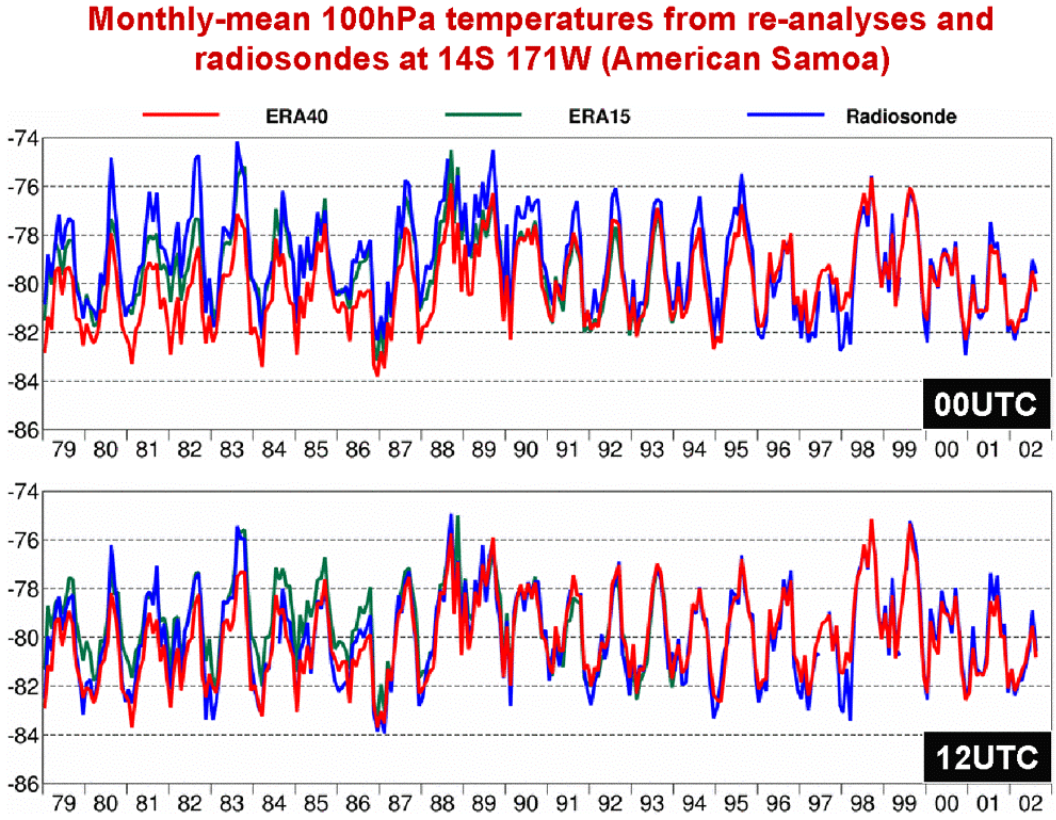

Figure 16: Monthly-mean ERA-40 and ERA-15 analyses of 100hPa temperature at 14oS 171oW, compared with the monthly mean radiosonde observations from Pago Pago International Airport (American Samoa), plotted separately for 00UTC and 12UTC.

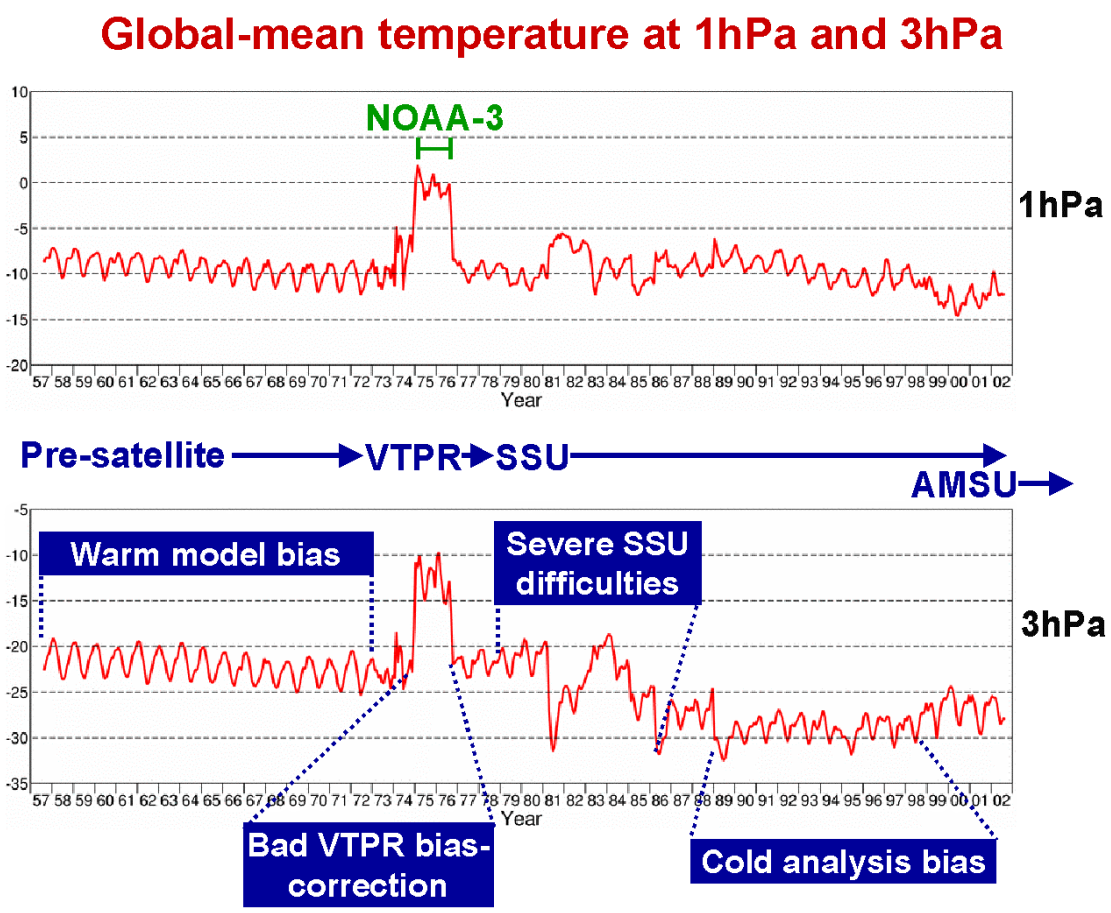

Figure 17: Time series of monthly- and global-mean ERA-40 temperature analyses at 1hPa and 3hPa.

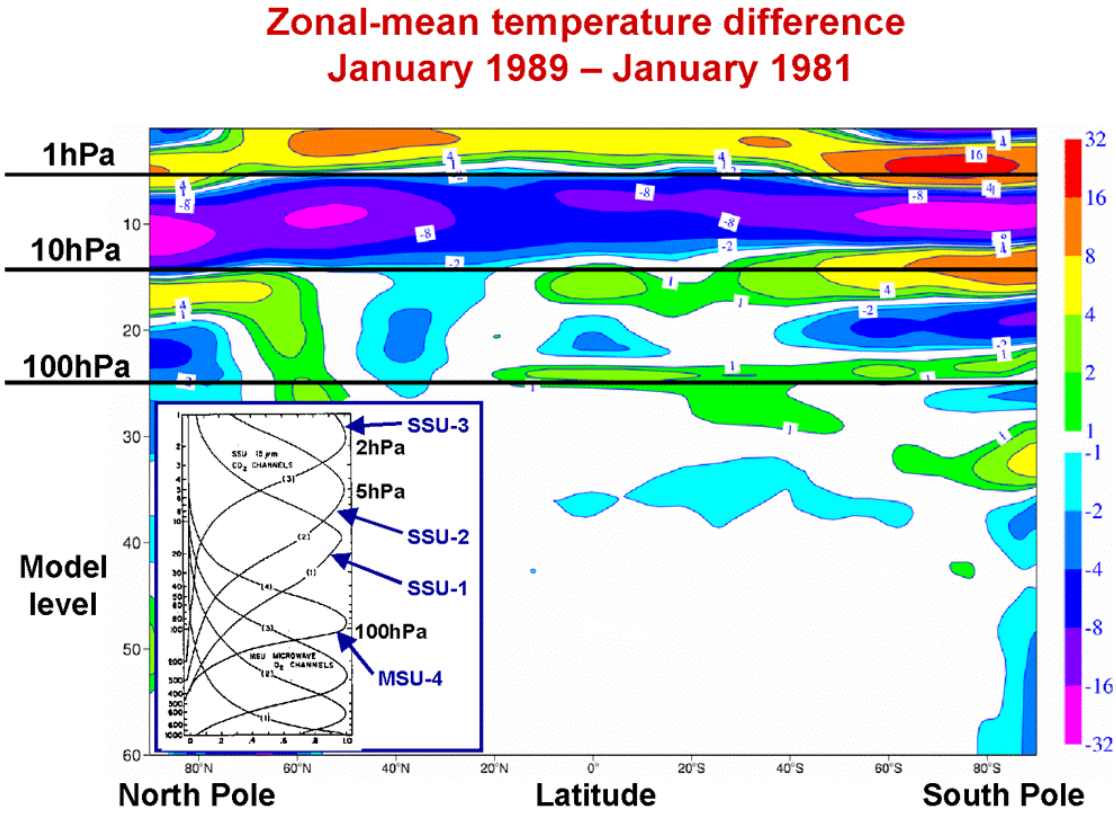

Figure 18: Zonal-mean difference between the January-mean ERA-40 temperature analyses for 1989 and 1981. The layers over which the measured SSU and MSU radiances are sensitive to temperature are also illustrated.

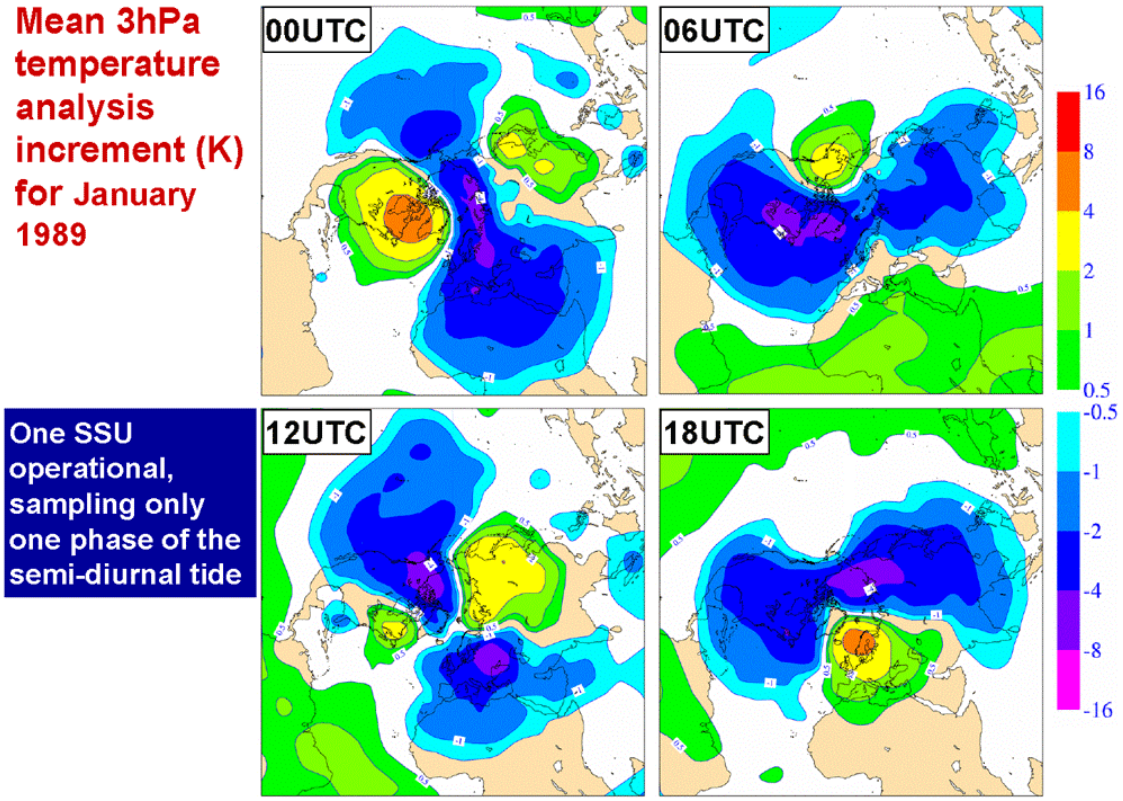

Figure 19: Mean analysis increments in 3hPa temperature for January 1989, shown separately for 00UTC, 06UTC, 12UTC and 18UTC.

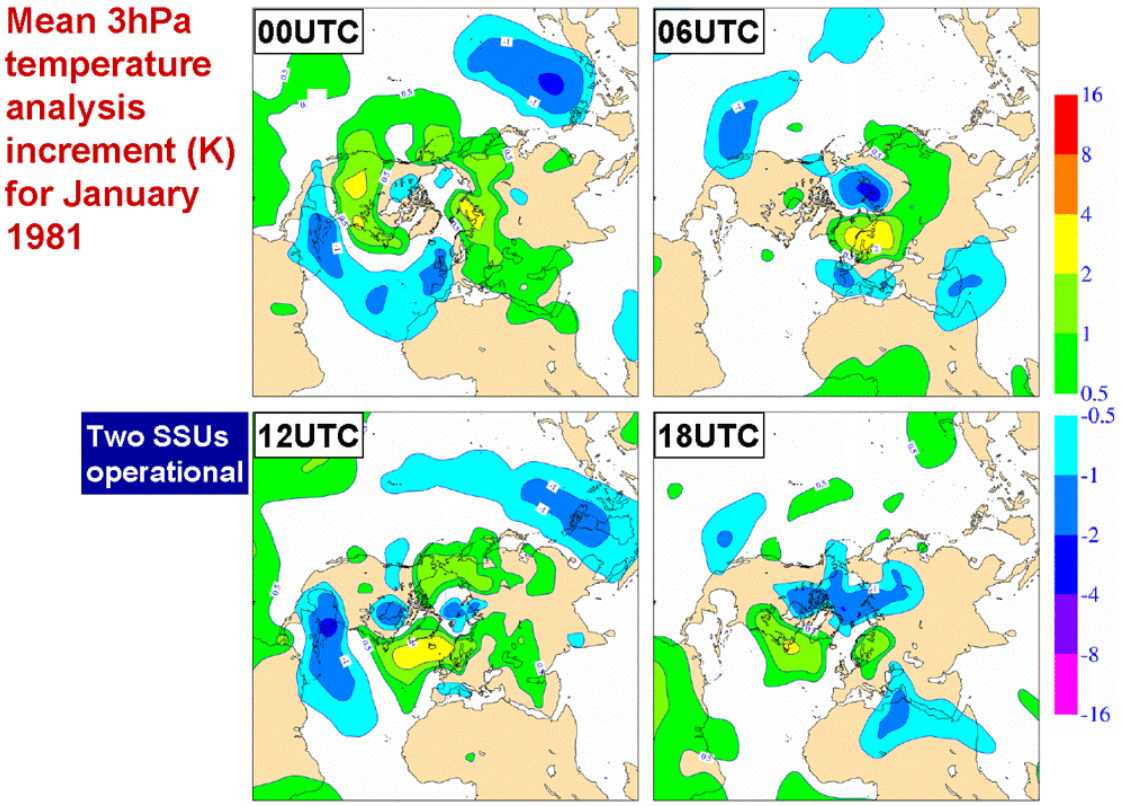

Figure 20: As Fig. 19, but for January 1981.

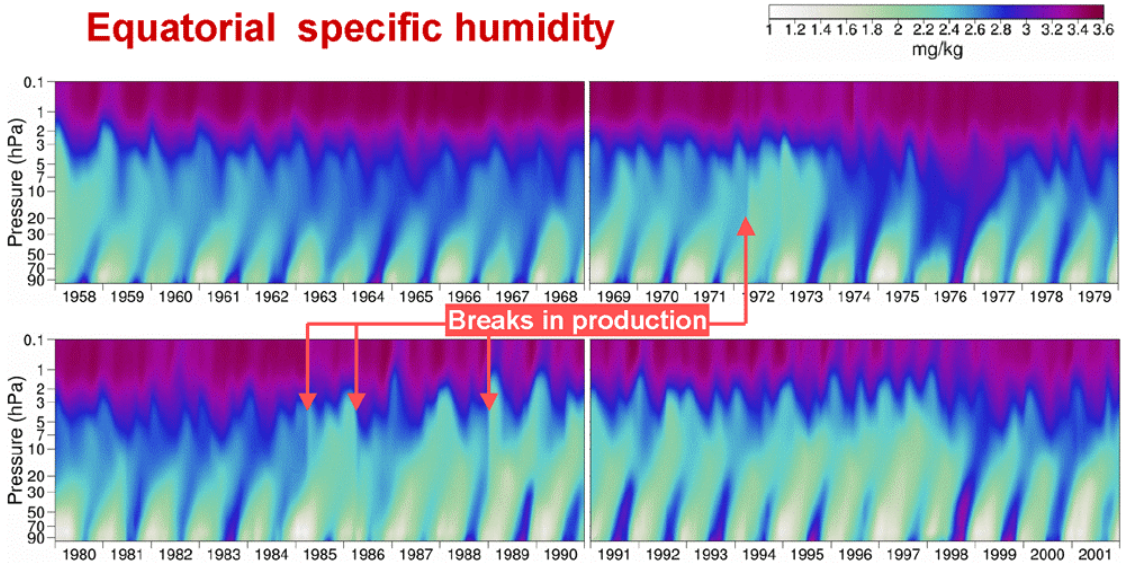

Figure 21: Time series of monthly-mean equatorial stratospheric specific humidity from ERA-40.

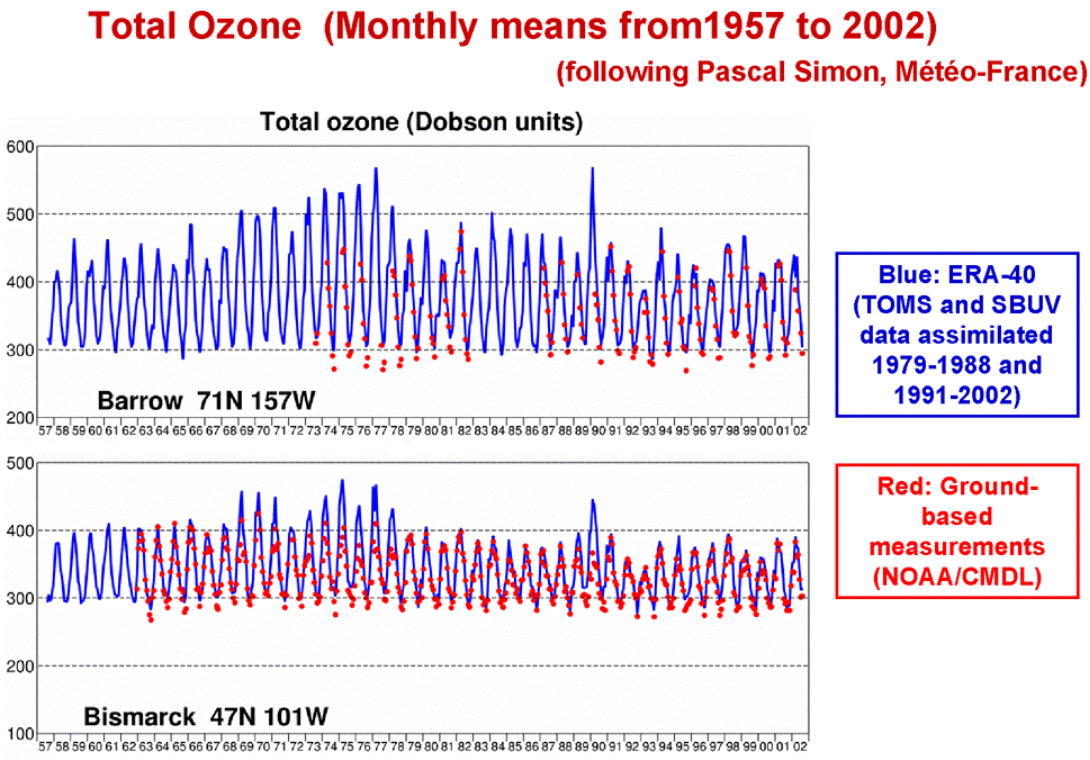

Figure 22: Time series of monthly-mean total column ozone from ERA-40 compared with ground-based measurements from the Barrow and Bismarck observing sites.

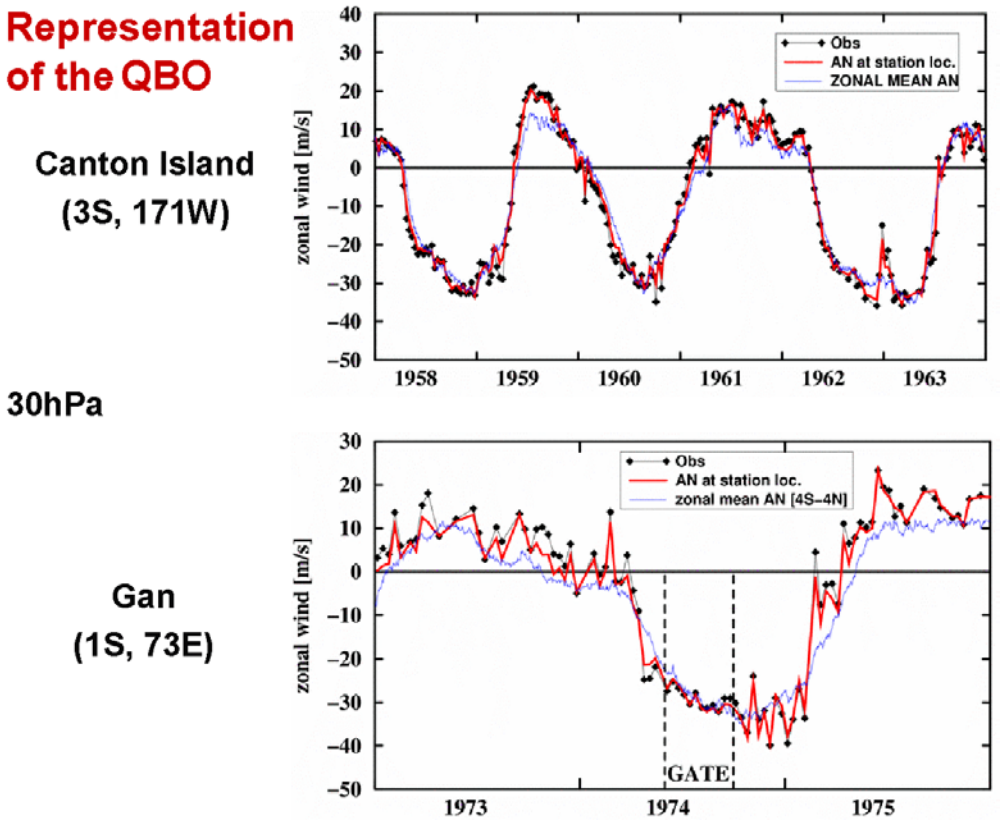

Figure 23: Time series of 10-day means of ERA-40 analyses of 30hPa zonal wind (point values at station locations and zonal means) compared with radiosonde measurements from Canton Island and Gan.

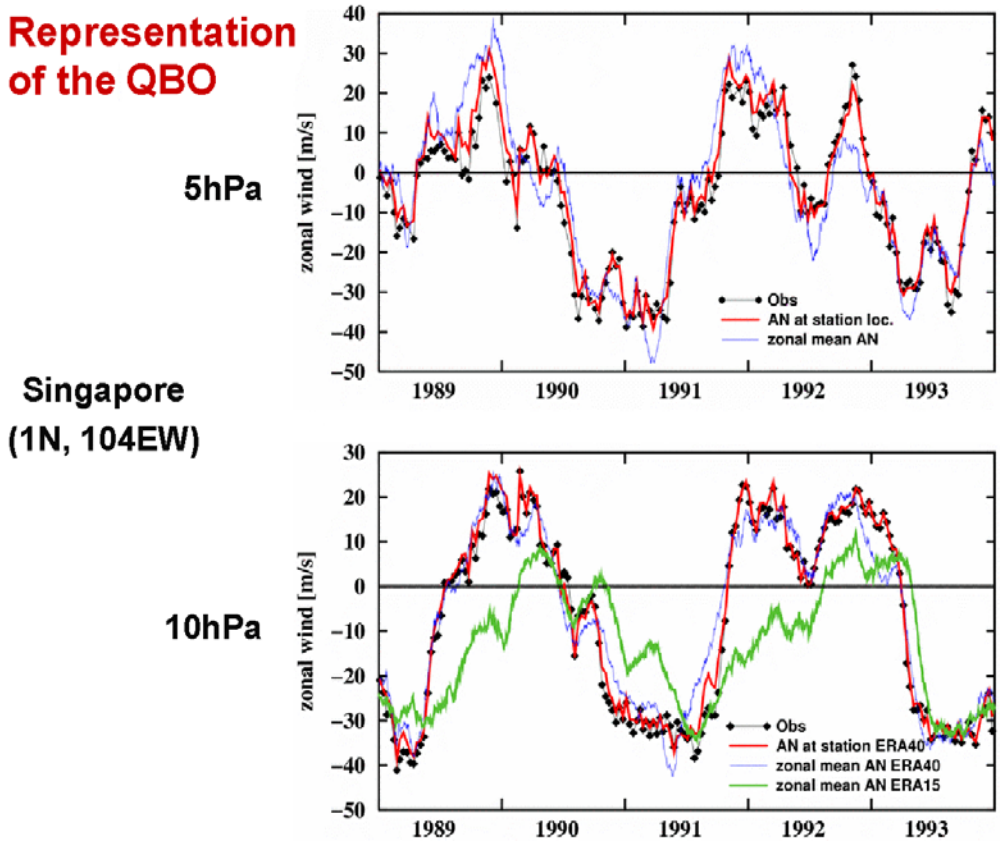

Figure 24: Time series of 10-day means of ERA-40 analyses of 10hPa and 5hPa zonal wind (point values at station location and zonal means) compared with radiosonde measurements from Singapore. ERA-15 results are also shown for the zonal mean at the 10hPa level.